Solvent and distance dependent charge separation in rigid trichromophoric systems

Roest, M.R.; Verhoeven, J.W.; Schuddeboom, W.; Warman, J.M.; Lawson, J.M.; Paddon-Row, M.N.

Solvent and Distance Dependent Charge Separation in Rigid Trichromophoric Systems

Martin R. Roest,[†] Jan W. Verhoeven,*,[†] Wouter Schuddeboom,[§]
John M. Warman,*,[§] James M. Lawson,[‡] and Michael N. Paddon-Row*,[‡]

Contribution from the Laboratory of Organic Chemistry, University of Amsterdam, Nieuwe Achtergracht 129, 1018 WS Amsterdam, The Netherlands, Interfaculty Reactor Institute, Delft University of Technology, Mekelweg 15, 2629 JB Delft, The Netherlands, and School of Chemistry, University of New South Wales, Sydney, NSW 2052, Australia
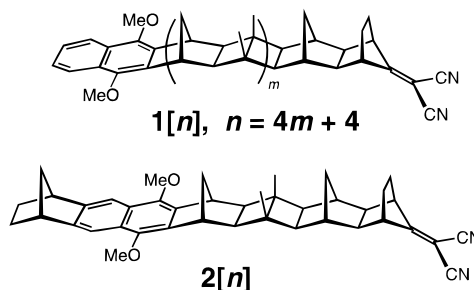
Received September 25, 1995[⊗]

Abstract: Transient absorption and time-resolved microwave studies have been carried out on a series of D(onor)$_2$−[bridge]−D(onor)$_1$−[bridge]−A(cceptor) compounds, in which a dimethoxynaphthalene (DMN) primary donor (D$_1$) and a dicyanovinyl (DCV) acceptor are separated by a rigid norbornylogous bridge eight σ-bonds in length and an *N,N*-dimethylaniline secondary donor (D$_2$) is separated from D$_1$ by a norbornylogous bridge of variable length (four, six, or eight σ-bonds). The identity of the charge-separated state populated upon photoexcitation, *i.e.*, from D$_1$ to A or from D$_2$ to A, depends on the solvent polarity and the length of the bridge separating both donor chromophores. It was found that the final charge-separated state is formed on a (sub)nanosecond time scale, whereas charge recombination shows strong solvent dependence, due to "inverted region" behavior.

Introduction

The series of donor−[bridge]−acceptor dyad systems, **1[*n*]**, comprising rigid hydrocarbon polynorbornane−bicyclo[2.2.0]-hexane ("norbornylogous") bridges with an effective length of *n* σ-bonds (*n* = 4−13), has provided valuable insight into the nature of long-range intramolecular photoinduced electron transfer (ET) processes.[1,2] The eight-bond dyads **1[8]** and **2[8]** (see Chart 1) epitomize the efficacy by which the norbornylogous bridge mediates ET (by a through-bond mechanism). Thus, intramolecular ET from the locally excited dimethoxynaphthalene (DMN) donor group to the dicyanovinyl (DCV) group is found to take place with unit quantum efficiency within *ca.* 20 ps and showing only a slight solvent dependency[3] because it occurs in the nearly optimal region.[4] The lifetime of the resulting charge-separated (CS) state to charge recombination (CR) amounts to about 32 ns in benzene[3b] and decreases sharply in more polar media because the large energy gap involved gives it typical "inverted region" behavior. Increasing the length of the norbornylogous bridge results in an exponential decay in the rates of *both* charge separation and charge recombination processes. This is due to the fact that the magnitudes of the electronic coupling matrix elements for both charge separation and charge recombination follow an exponential decay with increasing bridge length.

Consequently, in the case of bichromophoric systems, increasing the longevity of the CS state, brought about by increasing the bridge length, is achieved at the expense of reduced quantum efficiency of formation of the CS state. For
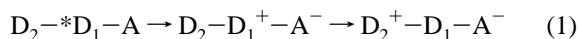
[†] University of Amsterdam.
[‡] University of New South Wales.
[§] Delft University of Technology.
[⊗] Abstract published in *Advance ACS Abstracts,* February 1, 1996.
(1) Warman, J. M.; Smit, K. J.; Jonker, S. A.; Verhoeven, J. W.; Oevering, H.; Kroon, J.; Paddon-Row, M. N.; Oliver, A. M. *Chem. Phys.* **1993,** *170,* 397 and references cited therein.
(2) Paddon-Row, M. N. *Acc. Chem. Res.* **1994,** *27,* 18 and references cited therein.
(3) (a) Oevering, H.; Paddon-Row, M. N.; Heppener, M.; Oliver, A. M.; Cotsaris, E.; Verhoeven, J. W.; Hush, N. S. *J. Am. Chem. Soc.* **1987,** *109,* 3258. (b) Paddon-Row, M. N.; Oliver, A. M.; Warman, J. M.; Smit, K. J.; de Haas, M. P.; Oevering, H.; Verhoeven, J. W. *J. Phys. Chem.* **1988,** *92,* 6958.
(4) Kroon, J.; Verhoeven, J. W.; Paddon-Row, M. N.; Oliver, A. M. *Angew. Chem., Int. Ed. Engl.* **1991,** *30,* 1358.

Chart 1. Structures of the Bichromophoric Model Compounds

1[*n*], *n* = 4*m* + 4

2[*n*]

example, although the lifetime of the CS state for the 12-bond bichromophore **1[12]** is *ca.* 20 times longer than that for the eight-bond system **1[8]**, the quantum efficiency for the formation of the CS state in **1[12]** is only 75% (compared to 100% efficiency in **1[8]**).[3b]

Notwithstanding the impressive rates of through-bond-mediated charge separation in bichromophoric systems, such as the **1[*n*]** series, it is clear that bichromophoric systems cannot meet the dual requirement of near unit efficiency for formation of the CS state *and* suitable longevity of that state toward charge recombination (*ca.* milliseconds). Satisfying this dual requirement is a necessary condition for the successful design of molecular electronic devices, such as molecular photovoltaic cells.[5]

This requirement can be met by using multichromophoric systems, *i.e.*, triads, tetrads, pentads, etc., that constitute a gradient of redox centers arranged within a spatially well-defined array. The principle behind this strategy is illustrated in eq 1 for the case of the covalently linked triad D$_2$−D$_1$−A, in which D$_1$ is initially locally excited.

$$D_2-{}^*D_1-A \rightarrow D_2-D_1{}^+-A^- \rightarrow D_2{}^+-D_1-A^- \qquad (1)$$

In this system, the ET process takes place in a sequence of rapid "hops" between adjacent chromophores that are spanned by a bridge that is short enough to guarantee that the hop occurs

(5) (a) Gust, D.; Moore, T. A.; Moore, A. L. *Acc. Chem. Res.* **1993,** *26,* 198. (b) Wasielewski, M. R. *Chem. Rev.* **1992,** *92,* 435.

Chart 2. Structures of the *Syn* and *Anti* Isomers of the Trichromophoric Compounds Synthesized[a]

[4:8]–*syn*   {14.9}

[4:8]–*anti*   {19.4}

[6:8]–*syn*   {16.8}

[6:8]–*anti*   {21.7}

[8:8]–*syn*   {17.1}

[8:8]–*anti*   {23.8}
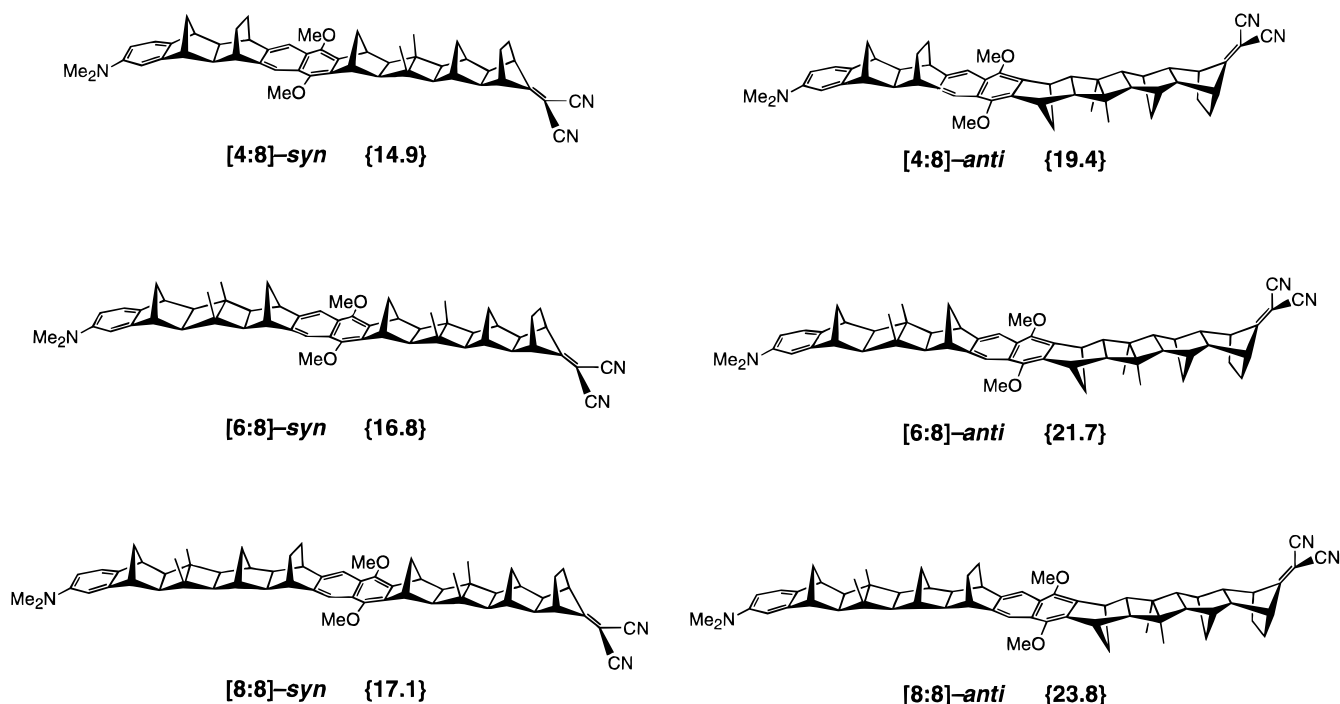
[a] In braces is given the center-to-center distance in angstroms between the terminal chromophores, measured from the central carbon atom of the dicyanovinyl acceptor to the center of the aniline ring.

with near unit efficiency. The final result is charge separation over a sufficiently large distance that the unwanted charge recombination step becomes acceptably slow enough. Indeed, several elegant studies have verified the viability of the multichromophore approach to the design of long-lived charge-separated molecular species.[5,6]

Encouraged by such reports, we have embarked on a systematic study of photoinduced ET processes in novel multichromophoric systems based on the norbornylogous bridge. These systems should offer several significant advantages over other polychromophoric systems studied to date. In particular, the ease by which the length and configuration of the bridge can be altered confer upon norbornylogous-based multichromophoric systems the potential for providing important insight into the factors governing both the dynamics of stepwise

Chart 3. MM2-Optimized Structures of the [4:8]-*syn* and [4:8]-*anti* Trichromophores

[4:8]–*syn*   [4:8]–*anti*
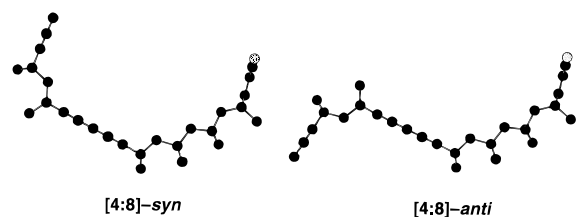
photoinduced ET processes leading to the formation of giant CS states and the subsequent lifetimes of these states toward charge recombination.

The first such multichromophoric systems successfully synthesized by the UNSW group are the triads shown in Chart 2.[7] Each triad contains the eight-bond DMN−DCV bichromophoric component to which is appended a second norbornylogous bridge of variable length (four, six, or eight σ-bonds) that is terminated by an *N,N*-dimethylaniline (DMA) secondary donor moiety. An interesting feature of these systems is that each trichromophore possesses two noninterconverting diastereomeric *syn* and *anti* forms, each of which has been isolated. That these diastereomers have quite different shapes is clearly illustrated by the profiles of the MM2-optimized structures of the [4:8]-*anti* and [4:8]-*syn* diastereomers (Chart 3). The *syn* diastereomer has a U‑shaped profile, whereas the *anti* stereoisomer has an extended or S-shaped profile. This difference in geometry results in a significantly larger center-to-center distance between the terminal chromophores in the "S-shaped" *anti* isomer compared to the *syn* isomer.[8,9]

As we have recently reported,[8,10] flash photolysis of [4:8]-*anti* in di-*n*-butyl ether leads to complete charge separation to produce the giant CS state, namely, DMA•+[4]DMN[8]DCV•−

(6) (a) Gust, D.; Moore, T. A.; Makings, L. R.; Liddell, P. A.; Nemeth, G. A.; Moore, A. L. *J. Am. Chem. Soc.* **1986**, *108*, 8028. (b) Sakata, Y.; Tatemitsu, H.; Bienvenue, E.; Seta, P. *Chem. Lett.* **1988**, 1625. (c) Collin, J. P.; Guillerez, S.; Sauvage, J.-P.; Barigelletti, F.; De Cola, L.; Flamigni, L.; Balzani, V. *Inorg. Chem.* **1991**, *30*, 4230. (d) Osuka, A.; Najata, T.; Maruyama, K.; Mataga, N.; Asahi, T.; Yamazaki, I.; Nishimura, Y. *Chem. Phys. Lett.* **1991**, *185*, 88. (e) Mecklenburg, S. L.; Peek, B. M.; Erickson, B. W.; Meyer, T. J. *J. Am. Chem. Soc.* **1991**, *113*, 8540. (f) Cooley, L. F.; Larson, S. L.; Elliott, C. M.; Kelley, D. F. *J. Phys. Chem.* **1991**, *95*, 10694. (g) Larson, S. L.; Cooley, L. F.; Elliott, C. M.; Kelley, D. F. *J. Am. Chem. Soc.* **1992**, *114*, 9504. (h) Brouwer, A. M.; Mout, R. D.; Maassen, P. H.; van den Brink, M.; van Ramesdonk, H. J.; Verhoeven, J. W.; Jonker, S. A.; Warman, J. M. *Chem. Phys. Lett.* **1991**, *186*, 481. (i) Brouwer, A. M.; Eijckelhoff, C.; Willemse, R. J.; Verhoeven, J. W.; Schuddeboom, W.; Warman, J. M. *J. Am. Chem. Soc.* **1993**, *115*, 2988. (j) Wiederrecht, G. P.; Watanabe S.; Wasielewski, M. R. *Chem. Phys.* **1993**, *176*, 601. (k) Wasielewski, M. R.; Gaines, G. L., III; Wiederrecht, G. P.; Svec W. A.; Niemczyk, M. P. *J. Am. Chem. Soc.* **1993**, *115*, 10442. (l) Gust, D.; Moore, T. A.; Moore, A. L. *J. Am. Chem. Soc.* **1993**, *115*, 11141. (m) Osuka, A.; Yamada, H.; Maruyama, K.; Mataga, N.; Asahi, T.; Ohkohchi, M.; Okada, T.; Yamazaki, I.; Nishimura, J. *J. Am. Chem. Soc.* **1993**, *115*, 9439. (n) Ohkohchi, M.; Takahasi, A.; Mataga, N.; Okada, T.; Osuka, A.; Yamada, H.; Maruyama, K. *J. Am. Chem. Soc.* **1993**, *115*, 12137. (o) van Dijk, S. I.; Wiering, P. G.; van Staveren, R.; van Ramesdonk, H. J.; Brouwer, A. M.; Verhoeven, J. W. *Chem. Phys. Lett.* **1993**, *214*, 205. (p) Osuka, A.; Zhang, R. P.; Maruyama, K.; Ohno, T.; Nozaki, K. *Bull. Chem. Soc. Jpn.* **1993**, *66*, 3773. (q) Hung, S.-C.; Lin, S.; Macpherson, A. N.; DeGraziano, J. M.; Kerrigan, P. K.; Lidell, P. A.; Moore, A. L.; Moore, T. A.; Gust, D. *J. Photochem. Photobiol., A: Chem.* **1994**, *77*, 207. (r) Willemse, R. J.; Verhoeven, J. W.; Brouwer, A. M. *J. Phys. Chem.* **1995**, *99*, 5753.

(7) (a) Lawson, J. M.; Paddon-Row, M. N. *J. Chem. Soc., Chem. Commun.* **1993**, *21*, 1641. (b) Lawson, J. M.; Craig, D. C.; Oliver, A. M.; Paddon-Row, M. N. *Tetrahedron* **1995**, *52*, 3841.

(8) Lawson, J. M.; Paddon-Row, M. N.; Warman, J. M.; Schuddeboom, W.; Clayton, A. H. A.; Ghiggino, K. P. *J. Phys. Chem.* **1993**, *97*, 13099.

(henceforth designated by CT-2), in which the overall result is transfer of an electron from the DMA secondary donor group to the DCV acceptor. In benzene, however, this giant CS state is in equilibrium with another CS state, namely, DMA[4]-DMN$^{•+}$[8]DCV$^{•-}$ (henceforth designated by CT-1), in which only charge separation from the DMN primary donor to the DCV acceptor is taking place.[10]

In this paper, we present a more detailed account of our investigations on our trichromophoric systems. In particular, using a combination of time-resolved transient absorption (TA) spectroscopy and time-resolved microwave conductivity (TRMC), we have investigated photoinduced ET processes in the remaining two members of the *anti* series of diastereomers, namely, **[6:8]**-*anti* and **[8:8]**-*anti*. We also present a more extensive investigation into the solvent dependency of the dynamics of charge separation and charge recombination processes occurring in the *anti* series of trichromophores.

This paper is restricted to a study of the *anti* series of diastereomers because, somewhat surprisingly, preliminary measurements indicate that the dynamics of charge recombination from the CS states of the *syn* series of diastereomers are quite different from those of the corresponding *anti* series.[8,10] Investigations into the photophysics of the *syn* series are ongoing and will be reported at a later date.

Results and Discussion

Transient Absorption Spectroscopy. In the TA experiment the sample is excited at 308 nm with an XeCl excimer laser, after which the absorption spectrum of the populated transients is obtained by probing at right angles with a Xe flash lamp (see the Experimental Section). To obtain insight into the obtained spectra, the spectra of the separate radical cations of DMA and DMN and the radical anion of DCV were also obtained as described previously.[10]

The radical cation of a suitable DMA model was prepared[10] by cosensitization with biphenyl and dicyanonaphthalene and was found to have an absorption band at 490 nm. The radical cation of a DMN model was prepared[10,11] by oxidation with 2,3-dichloro-5,6-dicyanobenzoquinone/trifluoroacetic acid, and it was found to be stable for several days. Its absorption spectrum displays an intense band at 408 nm, together with two broad, less intense absorptions at 500 and 600 nm. The radical anion of DCV was obtained by intramolecular electron transfer quenching with DMA and shows an absorption shoulder around 350 nm.

Transient absorption spectra of **[n:8]**-*anti* (with n = 4, 6, 8) were taken in *n*-hexane, benzene, di-*n*-butyl ether, and tetrahydrofuran (THF). In these solvents the bichromophoric model compounds **1[8]** and **2[8]** undergo quantitative charge separation upon photoexcitation of the DMN chromophore within the time resolution of the apparatus (*i.e.*, <5 ns), yielding a spectrum equal to the sum of the DMN$^{•+}$ radical cation and DCV$^{•-}$ radical anion absorptions[10] (see Figure 1). Previous studies[3,11b] revealed that charge separation in **1[8]** takes place in 10−20 ps, whereas the rate of charge recombination displays a pronounced solvent polarity effect, varying from 17 ns in *n*-hexane to 40 and 49 ns in benzene and di-*n*-butyl ether, respectively.

(9) Unequivocal stereochemical assignment, *anti* or *syn*, to the diastereomers of the **[6:8]** system was obtained from the X-ray crystal structure determination of **[6:8]**-*syn*.[7b] Stereochemical assignments in the **[4:8]** and **[8:8]** systems are less certain and were made on the basis of matching physical properties (*i.e.*, TLC R_f values, photophysics, *vide infra*)[7b,8,10] of the isomers of these systems with those of **[6:8]**-*anti* and **[6:8]**-*syn*.

(10) Roest, M. R.; Lawson, J. M.; Paddon-Row, M. N.; Verhoeven, J. W. *Chem. Phys. Lett.* **1994**, *230*, 536.

(11) (a) Sep, W. Ph.D. Thesis, University of Amsterdam, Amsterdam, 1979. (b) Oevering, H. Ph.D. Thesis, University of Amsterdam, Amsterdam, 1988. (c) Kroon, J. Ph.D. Thesis, University of Amsterdam, Amsterdam, 1992.
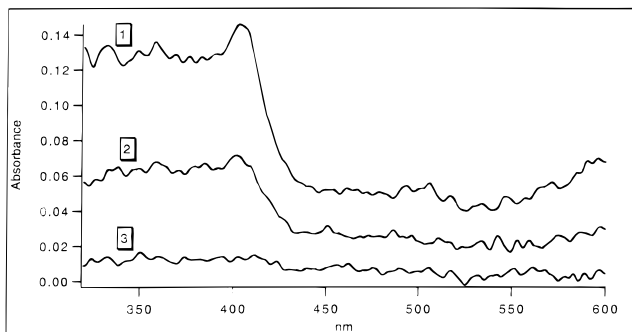
Figure 1. Transient absorption spectra of **2[8]** in di-*n*-butyl ether. Spectra taken (1) just after, (2) 10 ns after, and (3) 50 ns after laser pulse. The decay at 408 nm can be fitted to a monoexponential decay of 12 ns.
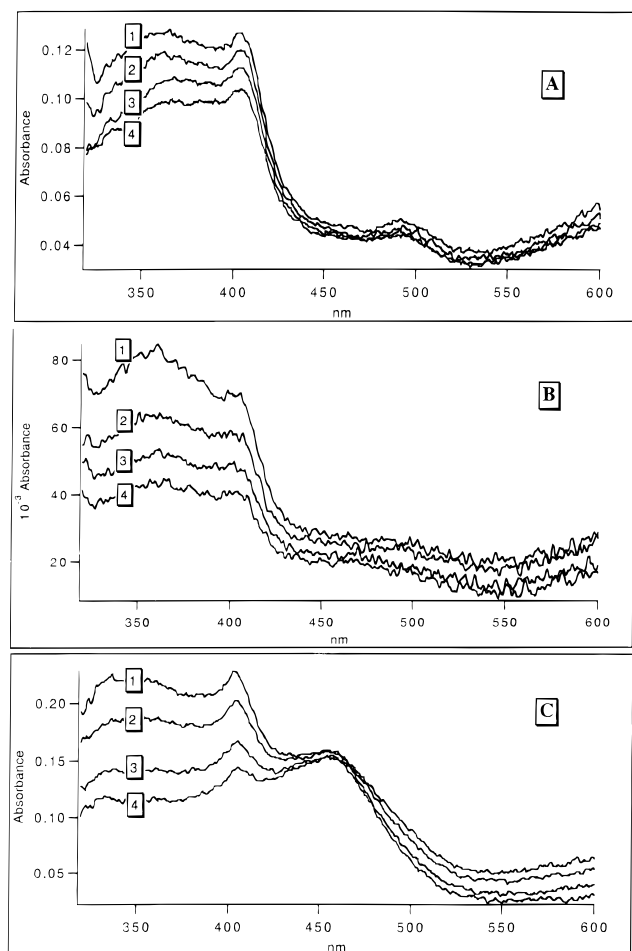

Figure 2. Transient absorption spectra of (A) **[4:8]**-*anti*, (B) **[6:8]**-*anti*, and (C) **[8:8]**-*anti* in *n*-hexane. Spectra taken (1) just after, (2) 4 ns after, (3) 8 ns after, and (4) 12 ns after laser pulse.

Upon photoexcitation of the triads **[n:8]**-*anti* in *n*-hexane, the TA spectra all show a strong absorption around 400 nm and a shoulder at *ca*. 350 nm. Since these features were also observed in the TA spectrum of **2[8]**, following flash photolysis, we conclude that only ET from the primary DMN donor to the DCV acceptor, to form the CT-1 state, is occurring in this solvent (Figure 2). The triad **[8:8]**-*anti* shows, apart from these radical ion absorptions, a strong triplet−triplet absorption located around 460 nm. The lifetime of the CT-1 state as measured from the absorption band around 400 nm is 26, 27, and 25 ns for **[4:8]**-*anti*, **[6:8]**-*anti*, and **[8:8]**-*anti*, respectively (Table 1). In benzene the TA spectrum corresponding to the CT-1 state is again observed following flash photolysis of **[6:8]**-*anti* and **[8:8]**-*anti*; however, **[4:8]**-*anti* yields a totally different TA spectrum

Table 1. Lifetimes (τ) Obtained from the Optical Spectroscopy Experiments in *n*-Hexane, *trans*-Decalin, Benzene, Di-*n*-butyl Ether, and THF for the Triads **[*n*:8]**-*anti* and the Bichromophoric Model Compounds **1[8]** and **2[8]** (In parentheses is given the major CT state formed is given)

	τ (ns)				
compd	*n*-hexane	*trans*-decalin	benzene	di-*n*-butyl ether	THF
1[8]	13[a] (CT-1)	61[a] (CT-1)	40[a] (CT-1)	49[a] (CT-1)	
2[8]	24[a] (CT-1)	72[a] (CT-1)	22[a] (CT-1)	13[b] (CT-1)	(CT-1)
[4:8]-*anti*	26[b] (CT-1)	73[a] (CT-1)	54[b] (CT-2)	73[b] (CT-2)	<5[b] (CT-2)
[6:8]-*anti*	27[b] (CT-1)	74[a] (CT-1)	22[a] (CT-1)	15[b] (CT-2)	20[b] (CT-2)
[8:8]-*anti*	25[b] (CT-1)	70[a] (CT-1)	17[a] (CT-1)	23[b] (CT-1)	(CT-2)

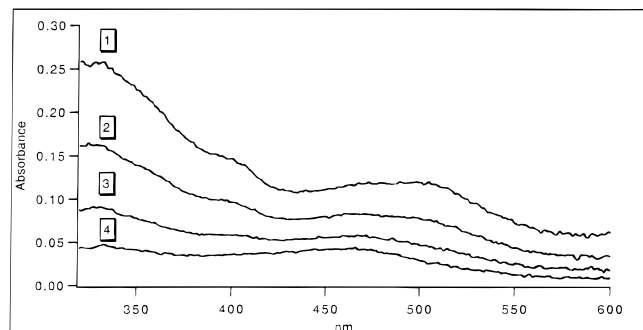[a] Determined from CT-1 fluorescence. [b] Determined from TA.

Figure 3. Transient absorption spectrum of **[4:8]**-*anti* in benzene (1) just after, (2) 25 ns after, (3) 50 ns after, and (4) about 100 ns after the laser pulse. The decay at 490 nm (as that at 350 nm) can be fitted to a monoexponential decay of 53 ns. The long-lived component is due to the absorption of the triplet state which has an infinite lifetime on this time scale.

Figure 4. Transient absorption spectrum of **[4:8]**-*anti* in di-*n*-butyl ether (1) just after, (2) 25 ns after, (3) 50 ns after, and (4) 100 ns after the laser pulse. The decay at 490 nm (as that at 350 nm) can be fitted to a monoexponential decay of 73 ns. The long-lived component is due to the absorption of the triplet state which has an infinite lifetime on this time scale.
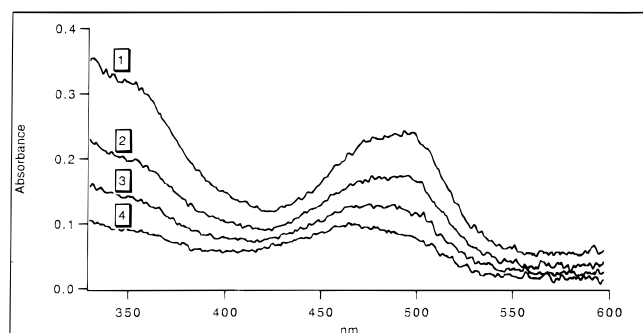
following flash photolysis (Figure 3) in which the strong 400 nm absorption band of DMN$^{\bullet+}$ is replaced by an intense absorption at *ca.* 490 nm. As was previously shown,[10] the 490 nm absorption band arises from the DMA$^{\bullet+}$ radical cation while the shoulder around 350 nm arises from the DCV$^{\bullet-}$ radical anion absorption. The lifetime of this fully charge-separated CT-2 species is found to be 54 ns. Also a minor contribution from the CT-1 state is present as can be seen from the small absorption which remains at 400 nm. Photoexcitation of **[4:8]**-*anti* in the more polar di-*n*-butyl ether solvent yields the spectrum corresponding to the giant charge-separated CT-2 state (Figure 4), with a lifetime of 73 ns. In the even more polar THF solvent, the TA spectrum of **[4:8]**-*anti* again indicates complete charge separation, but the lifetime of this CT-2 state shortens to <5 ns (Figure 5). The TA spectrum in di-*n*-butyl ether and THF solvents revealed no contribution from the CT-1 state.

The behavior of **[4:8]**-*anti* indicates that the second charge separation step (CT-1 → CT-2) becomes energetically feasible at solvent polarities equal to or exceeding that of benzene.
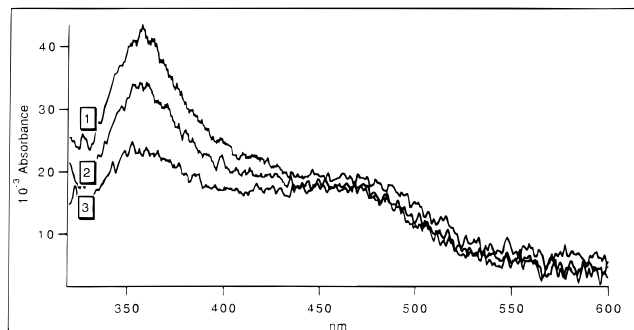

Figure 5. Transient absorption spectrum of **[4:8]**-*anti* in THF (1) just after, (2) 4 ns after, and (3) 8 ns after the laser pulse. The decay at 490 nm is too fast (<5 ns) to be fitted. On longer time scale, a long-lived component with an absorption at 470 nm remains which is due to the absorption of the triplet state and has an infinite lifetime on this time scale. Because of spectral overlap, it is left out for clarity.
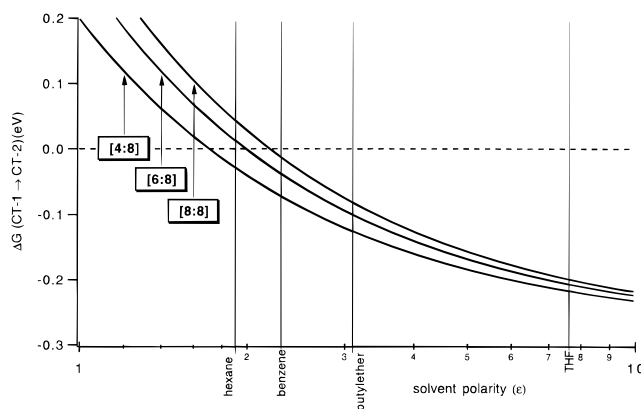

Figure 6. Calculated driving forces for the second-electron transfer step obtained with eq 2.

Applying the classical Born-type formulation for calculating ion pair energies, the Gibbs free energy for conversion of the initial DMA[*n*]DMN$^{\bullet+}$[8]DCV$^{\bullet-}$ (CT-1) species into the DMA$^{\bullet+}$[*n*]-DMN[8]DCV$^{\bullet-}$ (CT-2) species is given by:

$$\Delta G_{1,2} \text{ (eV)} = E_{ox}^{DMA} - E_{ox}^{DMN} - \frac{14.4}{\epsilon_s}\left(\frac{1}{R_2} - \frac{1}{R_1}\right) \quad (2)$$

In eq 2 R_1 and R_2 are the center-to-center charge separation distances in Å for the CT-1 and CT-2 states, respectively, while E_{ox}^{DMA} and E_{ox}^{DMN} are the one-electron oxidation potentials of the donors. It is assumed that the ionic radii of DMA$^{\bullet+}$ and DMN$^{\bullet+}$ are equal. Substitution of the appropriate electrochemical data ($E_{ox}^{DMA} = 0.73$ V and $E_{ox}^{DMN} = 1.01$ V, vs SCE[8]) and the distances obtained either from X-ray analysis (11.8 Å for **1[8]**) or from molecular modeling for the **[*n*:8]**-*anti* compounds (see Chart 2) leads to the driving forces which are plotted as a function of the solvent dielectric constant (ϵ_s) in Figure 6.

While these driving force values are very approximate, they nevertheless imply that the driving force associated with the second charge transfer step for **[6:8]**-*anti* in di-*n*-butyl ether is comparable to that for the same step for **[4:8]**-*anti* in benzene.
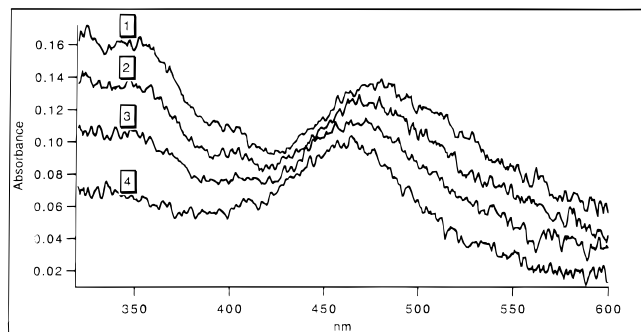
Figure 7. Transient absorption spectrum of **[6:8]**-*anti* in di-*n*-butyl ether (1) just after, (2) 2 ns after, (3) 10 ns after, and (4) 30 ns after the laser pulse. The decay at 490 nm (as that at 350 nm) can be fitted to a monoexponential decay of 13 ns. The long-lived component is due to the absorption of the triplet state which has an infinite lifetime on this time scale.

Figure 8. Transient absorption spectra of (A) **[6:8]**-*anti* and (B) **[8:8]**-*anti* in THF. Delays shown are 0, 4, 8, and 12 ns. The decay at 490 nm (as that at 350 nm) for **[6:8]**-*anti* can be fitted to a monoexponential decay of 20 ns. The long-lived component is due to the absorption of the triplet state wh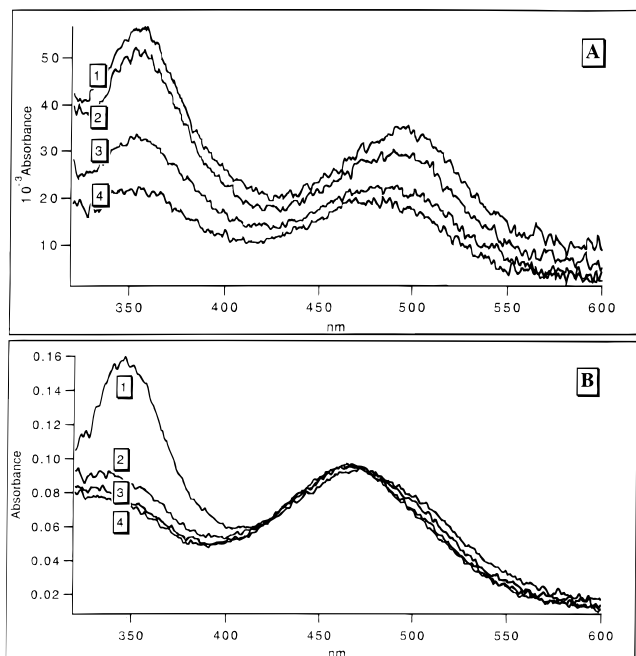ich has an infinite lifetime on this time scale. For **[8:8]**-*anti* the lifetime could not be fitted due to severe spectral overlap with a local triplet−triplet absorption. Only a shift from the DMA$^{\bullet+}$ to the local triplet absorption can be observed.

Indeed, flash photolysis of **[6:8]**-*anti* in this solvent yields a TA spectrum that is consistent with the formation of the giant charge-separated CT-2 state, together with a minor contribution from the partially charge-separated CT-1 state, whose presence is indicated by an absorption at 400 nm (see Figure 7). The lifetime found for the giant charge-separated CT-2 state is 15 ns. The **[8:8]**-*anti* isomer in di-*n*-butyl ether shows only evidence for formation of the partial charge-separated CT-1 state with a lifetime of 23 ns. In THF the fully charge-separated CT-2 state is formed for all three homologues with lifetimes of <5 ns for **[4:8]**-*anti* and 20 ns for **[6:8]**-*anti*. The lifetime of the CT-2 state for **[8:8]**-*anti* could not be determined accurately because the TA spectrum is masked by substantial DMN triplet−triplet absorption (Figure 8).

Time-Resolved Microwave Conductivity. As shown above, transient absorption spectroscopy provides a valuable tool for discriminating between the formation of the CT-1 and CT-2 states in the present trichromophoric systems. Unfortunately,

extensive spectral overlap occurs between these species and other transients, especially local triplet states, populated as part of the charge recombination processes. The latter problem can be avoided by resorting to the time-resolved microwave conductivity technique.[12,13] This method enables the specific detection of dipolar species, thereby allowing quantification of their decay kinetics and of the magnitude of their dipole moment, irrespective of the presence of other, nondipolar transients, such as locally excited triplets. A drawback of the TRMC technique is its confinement to the use of nondipolar solvents, which therefore excludes di-*n*-butyl ether and THF which were employed for the TA experiments in order to induce conversion from the CT-1 to the CT-2 states in **[6:8]**-*anti* and **[8:8]**-*anti*. However, a strongly solvating medium which can be conveniently employed in TRMC studies is 1,4-dioxane (ϵ_s = 2.21). Although 1,4-dioxane is known to behave as a more polar solvent than would appear from its dielectric constant, it still may not be sufficiently strong to enable complete population of the CT-2 state for **[6:8]**-*anti* and **[8:8]**-*anti* (see Figure 6).

TRMC transients observed for the three trichromophores in three solvents (*trans*-decalin, benzene and 1,4-dioxane) are shown in Figure 9. In all cases the rise of the signals follows the integrated laser pulse (fwhm = 7 ns) in accord with the expected sub-nanosecond charge separation kinetics.

In the nonpolar *trans*-decalin solvent, the TRMC signal decays with $\tau = 60 \pm 5$ ns for all trichromophores studied. This is similar to the lifetimes for the charge-separated states of the bichromophores **1[8]** and **2[8]** (see Table 2). Also, the dipole moments calculated from the TRMC experiments (see the Experimental Section) are constant within the experimental accuracy (62 ± 5 D). These values correspond to charge separation over 12.9 Å and therefore confirm the dominant, or even exclusive, formation of the CT-1 state in all cases.

The lifetimes of the CT-1 states for **1[8]** and **2[8]** are significantly longer than those determined by transient absorption measurements carried out in *n*-hexane. This phenomenon is known to occur in nonpolar solvents[14] and has been attributed to the occurrence of thermal back-electron transfer to the locally excited donor state; this is a feasible process for the eight-bond bichromophore because of the near degeneracy of the locally excited state and the CT state in this system in nonpolar solvents. For comparison with the TRMC data, the lifetimes of the compounds studied were also determined by fluorescence decay in *trans*-decalin and are given in Table 1.

In benzene, the behavior of **[4:8]**-*anti* and, to a lesser degree, also that of **[6:8]**-*anti* deviates significantly from that of the model bichromophoric systems **1[8]** and **2[8]** (see Table 2). Both **1[8]** and **2[8]** produce TRMC-determined dipole moments corresponding to the CT-1 states, although the lifetimes of these states are significantly shorter ($\tau = 28$ ns) than in *trans*-decalin ($\tau = 70$ ns). The behavior of **[8:8]**-*anti* in benzene was similar to that of the model systems; only the CT-1 state was observed, and it possesses a dipole moment of 65 D and a lifetime of $\tau =$ 24 ns. In contrast, the dipole moments of the charge-separated states resulting from flash photolysis of **[4:8]**-*anti* and **[6:8]**-*anti* are very large, 92 and 83 D, respectively. This is consistent with near complete formation (>97%)[15] of the CT-2 state for **[4:8]**-*anti* (predicted dipole moment based on a point charge model of 93 D) and partial formation of the CT-2 state (*ca.*

(12) de Haas, M. P.; Warman, J. M. *Chem. Phys.* **1982**, *73*, 35.

(13) Schuddeboom, W. Ph.D. Thesis, Delft University of Technology, Delft, 1994.

(14) Warman, J. M.; Smit, K. J.; Jonker, S. A.; Verhoeven, J. W.; Oevering, H.; Kroon, J.; Paddon-Row, M. N.; Oliver, A. M. *Chem. Phys.* **1993**, *170*, 359.

(15) The dipole moment of the CT-1 state ($R_c = 11.8$ Å) is estimated to be 57 D. Using this value, we can estimate the contribution from CT-1 and CT-2 states from $\mu^2 = x\mu_1^2 + (1 - x)\mu_2^2$.
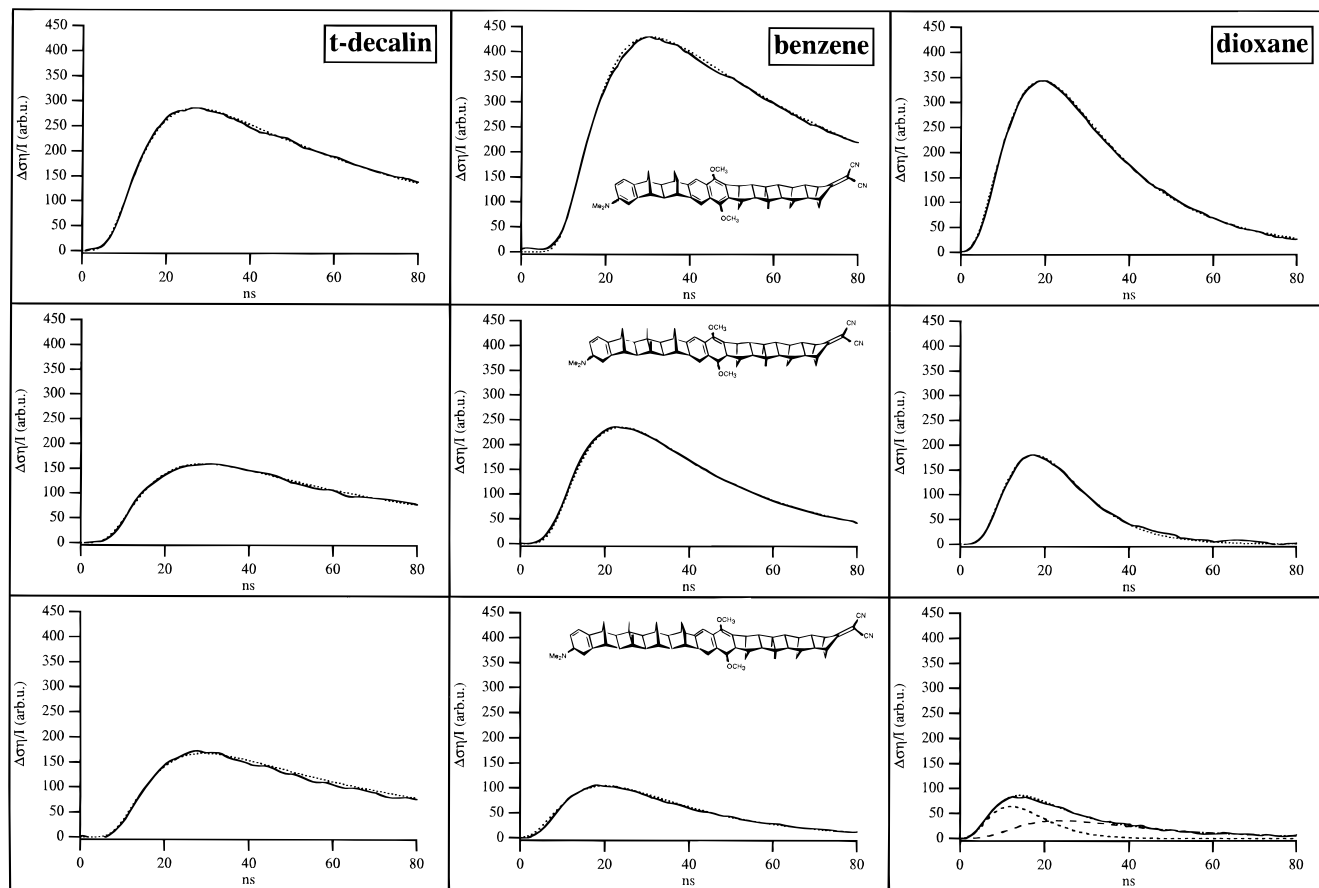
Figure 9. TRMC traces of **[4:8]**-*anti*, **[6:8]**-*anti*, and **[8:8]**-*anti* in *trans*-decalin, benzene, and 1,4-dioxane.

Table 2. Lifetimes (τ) and Dipole Moments (μ) Obtained from the TRMC Experiments in *trans*-Decalin, Benzene, and 1,4-Dioxane for the Triads **[n:8]**-*anti* and the Bichromophoric Model Compounds **1[8]** and **2[8]**

compd	τ (ns) (μ, D)		
	trans-decalin	benzene	1,4-dioxane
1[8]	58 (63)	32 (55)	2.5 (59)
2[8]	70 (59)	28 (55)	4 (63)
[4:8]-*anti*	62 (65)	64 (92)	20 (97)
[6:8]-*anti*	60 (56)	29 (83)	9 (94)
[8:8]-*anti*	55 (63)	24 (65)	4 (82)

50%) for **[6:8]**-*anti* (predicted dipole moment of 104 D). The lifetimes of the transient dipoles of **[4:8]**-*anti* and **[6:8]**-*anti* are 64 and 29 ns, respectively; the former is enhanced more than 2-fold, with respect to the bichromophoric reference systems, whereas the latter shows no enhancement. These findings are consistent with the conclusions drawn from the TA experiments, namely, that in benzene solvent the CT-2 state of **[4:8]**-*anti* becomes nearly completely populated. However, the TRMC results also show that significant population of the CT-2 state of **[6:8]**-*anti* occurs in benzene. The latter could not be detected from the TA spectra, probably due to strong spectral overlap of the DMA radical cation absorption, located at 490 nm, and the local triplet absorptions of DMA and DMN, which are located at 460 and 450 nm, respectively. These local triplet states can be formed upon charge recombination in yields depending on the trichromophore and the solvent.

For the **[4:8]**-*anti* system, both the predominant contribution made by the CT-2 state to the TRMC signal and its long lifetime indicate that the CT-2 state is formed essentially quantitatively from the CT-1 state, and that the reverse process, CT-2 → CT-1, is relatively slow, although the TA data indicate that partial equilibration is occurring. Interestingly, significant and rapid equilibration between the CT-1 and CT-2 states can be

concluded to occur for **[6:8]**-*anti* in benzene. This leads to an average dipole moment that significantly exceeds that expected for the CT-1 state, but the overall lifetime indicates that charge recombination is taking place largely via the CT-1 state.

As reported earlier,[8] the lifetime of the CT-1 states for the model bichromophoric compounds **1[8]** and **2[8]** typically drops by almost 1 order of magnitude upon changing the solvent from benzene to 1,4-dioxane (see Table 2); this is in qualitative accord with the "inverted region" effect expected upon diminishing the energy gap between the CT state and the ground state.

As expected, in 1,4-dioxane the transient dipole moment for **[4:8]**-*anti* again indicates complete population of the CT-2 state, although this state is only 75% populated for **[6:8]**-*anti*. The much longer lifetime of the CT-2 state for **[4:8]**-*anti*, compared to the model systems (20 ns vs 2.5−4 ns) proves that reversal from CT-2 to CT-1 is slow. However, although the lifetime of the CT state for **[6:8]**-*anti* is still considerably longer than that for the bichromophores, it is significantly shorter than that for **[4:8]**-*anti*. Thus, reversal of the CT-2 state to the CT-1 state still appears to be an important decay path for **[6:8]**-*anti* in 1,4-dioxane. Parenthetically, we note that the TA data (Table 1) reveal that in the more polar THF solvent, the CT-2 lifetime of **[6:8]**-*anti* exceeds that of **[4:8]**-*anti*, which is to be expected from the larger charge separation distance in the former molecule under conditions where reversal via CT-1 is energetically unfavorable. The behavior of **[8:8]**-*anti* in 1,4-dioxane is rather complex as its TRMC signal shows biexponential decay. It appears likely that also in this case the CT-2 state is partially populated but that its equilibration with the CT-1 state is sufficiently slow to lead to complex decay kinetics.

Based on all of the TA and TRMC data, the kinetic scheme depicted in Figure 10 can be derived. Upon excitation of the ground state to the locally excited state, direct relaxation to the ground state can occur (k_{1d}). Competing with this decay process
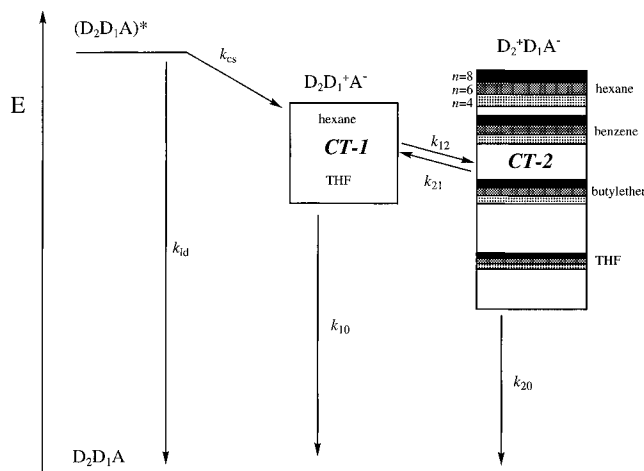
Figure 10. Schematic representation of the energy levels in the triads DMA[*n*]DMN[8]DCV depending on the solvent dielectric constant and DMA−DMN bridge length, *n*.

is charge separation to yield the CT-1 state, whose formation characteristics should be the same for all **[*n*:8]** trichromophores studied. This state shows solvent dependency as indicated by the height of the box. This state could either suffer charge recombination, to yield the ground state (k_{10}), depending on the solvent polarity, or undergo a second electron transfer step (k_{12}), yielding a second charge transfer state, CT-2. The energy of this giant charge-separated state not only depends on solvent polarity (which is more pronounced than for the CT-1 state due to the bigger dipole moment) but also shows a marked dependence on the DMA−DMN bridge length *n*, which is indicated in Figure 10 by the variously shaded areas. The CT-2 state can either undergo direct charge recombination to the ground state or, when the CT-1 and CT-2 states are nearly degenerate, undergo electron transfer from CT-2 to CT-1 (k_{21}). All decay paths to the ground state can in principle also lead to the formation of a local triplet state,[16] but these are omitted from the figure for reasons of clarity.

Conclusions

From both TA and TRMC experiments, it may be concluded that complete two-step charge separation in the triads **[4:8]**-*anti*, **[6:8]**-*anti*, and **[8:8]**-*anti* depends on the solvent polarity. In satured hydrocarbon solvents only charge separation from DMN to DCV occurs to form the CT-1 state, whereas in more polar solvents complete charge separation from DMA to DCV, to form the CT-2 state, takes place. The solvent polarity required to make this second step favorable increases with increasing bridge length between the DMA and DMN chromophores. The solvent polarity for which the second charge separation step occurs is predicted reasonably well from free energy calculations employing an ion pair model (Figure 6).

An important but somewhat annoying consequence of the polarity dependence of the CT-1 → CT-2 conversion is that extension of the bichromophoric systems to trichromophoric systems results only in a small increase in the lifetime of the charge-separated state. Thus, the lifetime of the CT-1 state in nonpolar solvents equals or exceeds that of the CT-2 state which can only be created in more polar solvents. On the other hand, in the more polar solvents, the CT-2 state has—as expected from the larger charge separation distance—a significantly longer lifetime than the CT-1 state in the same solvent (*cf.* **2[8]** and

[4:8]-*anti* in benzene and in 1,4-dioxane; Table 2); also the lifetime of the CT-2 state increases upon increasing the bridge length provided that a sufficiently polar solvent is chosen in order to prevent rapid return of CT-2 to CT-1 (*cf.* **[4:8]**-*anti* and **[6:8]**-*anti* in THF).

Finally, the nanosecond TA and TRMC results indicate that formation of both the CT-1 and CT-2 states (when energetically feasible) occurs on a sub-nanosecond time scale. Further investigations to quantify these kinetics with (sub)picosecond spectroscopy are presently in progress.[17,18] For the *syn* isomers, not only the formation but also the recombination kinetics are very rapid, as discussed before.[8,10] We are currently investigating those factors that are involved in these processes.

Experimental Section

Transient absorption spectra were obtained using a Lumonics EX700 XeCl excimer laser (308 nm) as the excitation source and a 450 W high-pressure Xe arc, pulsed with a Müller Elektronik MSP05 pulser to enhance its brightness during the observation time gate of the detector, in right angle geometry as probe light. The probe light, after passing through the sample cell, was collected by an optical fiber and fed into a Jarrel-Ash monospec 27 model 1234 spectrograph in which the light was dispersed by a grating (150 grooves/mm) onto an MCP-intensified diode array detector (EG&G 1421G, 25 mm, 1024 diodes). With this setup a spectral range of about 600 nm was covered with a bandwidth of 7 nm (250 μm slit). The detector was gated at 5 ns by an EG&G 1302 pulse generator, and the start of the time window was delayed in 2 or 5 ns increments relative to the laser pulse to obtain subsequent spectra across the total decay time of the transients studied. The timing of the laser, the probe light, and the optical multichannel analyzer (OMA) gate pulse was controlled by an EG&G OMA III Model 1460 console with a 1303 pulse delay generator and a digital delay generator (EG&G 9650). Spectra were averaged over 10−20 pulses for each delay to improve the signal to noise ratio.

Fluorescence lifetimes were determined by exciting the sample using a Lumonics EX700 XeCl excimer laser (308 nm, fwhm *ca.* 8 ns) and monitoring the fluorescence signal at right angle by a RCA C-31025C photodiode via a Zeiss MQ II monochromator. The signal of the detector was fed into a Tektronix TDS684A oscilloscope, triggered by a photodiode that detects the laser light pulse.

Samples were prepared in *n*-hexane (Merck, Uvasol), *trans*-decalin (Fluka, Purum; washed with H_2SO_4 and distilled from LiAlH), benzene (Merck, Uvasol), di-*n*-butyl ether (Merck; 99+%, washed with H_2SO_4 and distilled from NaH), or THF (Merck, Uvasol) to a concentration yielding A_{1cm}(308 nm) ≈ 1.0−1.5 (*ca.* 10^{-4} M) for transient absorption or A_{1cm}(308 nm) ≈ 0.1−0.15 (*ca.* 10^{-5} M) for fluorescence. Transient absorption samples were degassed by several freeze−pump−thaw cycles, whereas the samples for fluorescence decay measurements were purged with argon for at least 15 min.

For TRMC measurements, dilute (*ca.* 10^{-4} M) solutions were deoxygenated with carbon dioxide. The solvents were *trans*-decalin (Fluka, Purum), benzene (Merck, Uvasol), or 1,4-dioxane (Fluka; UV Spectroscopic grade). Decalin and 1,4-dioxane were passed through a column of activated silica gel prior to use. Samples contained within a microwave cavity cell were flash photolysed using a 7 ns fwhm pulse of 308 nm light from a Lumonics HyperEx 400 excimer laser. Any transient change occurring in the microwave conductivity, $\Delta\sigma(\omega)$, of the solutions was monitored as a change in microwave power reflected by the cell. The TRMC technique and the method of data reduction have been described fully elsewhere.[12,13]

(16) For investigations of this topic, see *e.g.*: (a) Lim, B. T.; Okajima, S.; Chandra, A. K.; Lim, E. C. *Chem. Phys. Lett.* **1981**, *79*, 22. (b) Ulrich, T.; Steiner, U. E.; Föll, R. E. *J. Phys. Chem.* **1983**, *87*, 1873. (c) Van Haver, Ph.; Helsen, N.; Depaemelaere, S.; Van der Auweraer, M.; De Schryver, F. C. *J. Am. Chem. Soc.* **1991**, *113*, 6849. (d) Morais, J.; Hung, R. R.; Grabowski, J. J.; Zimmt, M. B. *J. Phys. Chem.* **1993**, *97*, 13138.

(17) Stammler, W. Ph.D. Thesis, University of Erlangen-Nürnberg, Erlangen, 1995.

(18) Schneider, S.; Roest, M. R.; Paddon-Row, M. N.; Verhoeven, J. W.; *et al.* Unpublished observations.